

Computer Simulations of Geodynamo, Mantle Convection, and Earthquake

Project Representative

Akira Kageyama The Earth Simulator Center, Japan Agency for Marine-Earth Science and Technology

Authors

Akira Kageyama ^{*1}, Masanori Kameyama ^{*1}, Masaki Yoshida ^{*1},
Mamoru Hyodo ^{*1} and Mikito Furuichi ^{*1}

^{*1} The Earth Simulator Center, Japan Agency for Marine-Earth Science and Technology

By the end of Fiscal year 2004, we have devised two powerful numerical tools for parallel computation in solid Earth simulations—Yin-Yang grid and ACuTE method. Based on these original ideas, we further developed our simulation models this fiscal year and applied them to the geodynamo and mantle convection simulations. We also developed an earthquake simulation model to estimate the upper mantle viscosity.

Keywords: geodynamo, mantle convection, ACuTE method, Yin-Yang grid, multigrid method

1. Development Yin-Yang Grid Method

If you knife along a baseball's seam, you will get a couple of patches by which the ball's spherical surface is covered in combination. The patches or pieces are identical, i.e., they have exactly the same size and shape. Each piece is symmetric in two perpendicular directions; up-down and right-left. We call this kind of spherical dissection with two identical and symmetrical pieces "yin-yang dissection" of a sphere. The seam of the baseball is an example of the yin-yang dissection. Inspired by the yin-yang dissection of a sphere, we proposed a spherical grid system called "Yin-Yang grid".

Since we described the Yin-Yang grid method in detail in our papers [*Kageyama and Sato, 2004, Kageyama et al., 2004, Kageyama, 2005a*] and in the last Report [*Kageyama et al., 2005*], here we shortly summarize its merits: It is an orthogonal system (since it is a part of the latitude [Lat-Lon] grid); The grid spacing is quasi-uniform (since we picked up only the low latitude region of the Lat-Lon grid); The metric tensors are simple and analytically known (since it is defined based on the spherical polar coordinates); Routines that involve only individual component grid can be recycled for two times (since Yin and Yang are identical); Routines that involve its counterpart component can also be recycled for two times (since Yin and Yang are complementary); And, finally; It suits to massively parallel computers (since the domain decomposition is straightforward). An example of Yin-Yang grid is shown in Fig. 1.

In this fiscal year, we found a general procedure to construct yin-yang dissections of a sphere [*Kageyama, 2005b*]. Based on the dissection, we pointed out the relation between

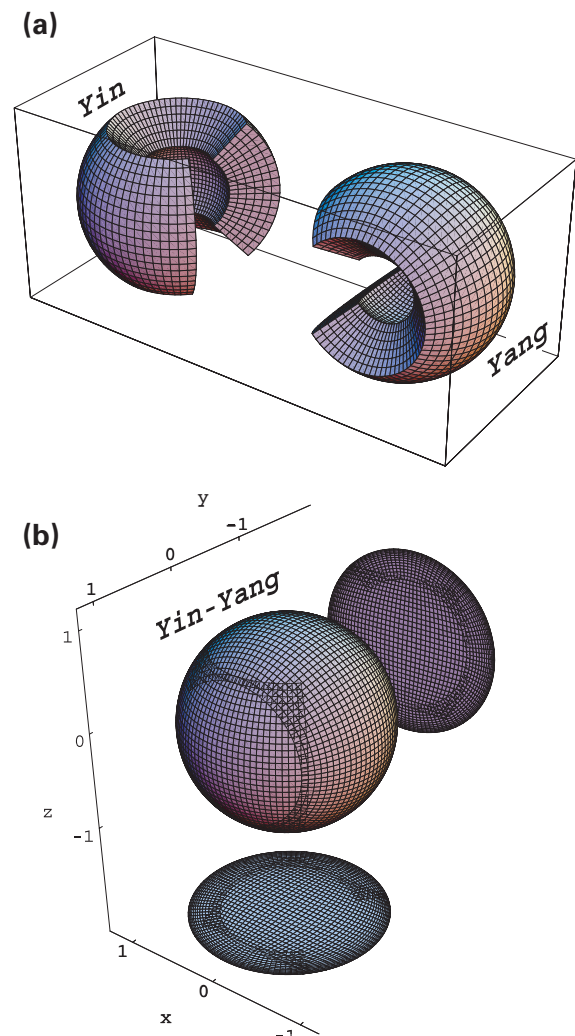


Fig. 1 Basic Yin-Yang grid. The Yin grid and Yang grid are combined to cover a spherical surface with partial overlap.

the yin-yang dissections and various versions of the Yin-Yang grids.

Another development of the Yin-Yang grid method in this year is the implementation of the multigrid method on the Yin-Yang grid, which was motivated by the improvement of the boundary condition of the magnetic field adopted in our Yin-Yang based geodynamo simulation code [Kageyama and Yoshida, 2005].

The purpose of this improvement is to incorporate the so-called vacuum boundary condition. In this boundary condition, the magnetic field generated by the MHD dynamo in the outer core (say, $r \leq 1$) is smoothly connected to the magnetic field B_V of the outer region $r > 1$ that is assumed to be an insulator. Therefore, B_V is written by the gradient of a potential field in $r \geq 1$.

The boundary condition of the potential is given by the radial component of the magnetic field on the boundary $r = 1$ which is obtained from the dynamo region ($r \leq 1$). Other components of the magnetic field on the surface are determined by the solution of the potential equation.

In order to solve this boundary value problem, we first apply a coordinate transformation of r ; $s = 1/r$. The potential problem is now converted into other boundary value problem defined *inside* a unit sphere $s \leq 1$.

To solve the boundary value problem for the potential for $s \leq 1$, we apply the multigrid method, which is practically the optimal way to solve this kind of boundary value problem. The base grid system is the Yin-Yang grid defined in the full spherical region including the origin. See Fig. 2. We adopt the full approximation storage algorithm of the multigrid method. The Jacobi method is used as the smoother. The V-cycle is repeated for a couple of times until we get the convergence. The internal boundary condition of each component grid (Yin and Yang) is set by mutual bi-cubic

interpolation at every grid level as indicated by white arrows in Fig. 2. Although, the code is not parallelized yet, its flat-MPI parallelization will be straightforward. We have combined this non-parallelized Yin-Yang multigrid solver of the vacuum potential ψ with the non-parallel version of the Yin-Yang geodynamo code. We have found that the vacuum field condition has been successfully implemented by this multigrid potential solver with almost the same computational cost (CPU time) as with the MHD solver part. This is a very promising result for further development.

2. Thermal state in the lower mantle with post-perovskite phase transition

Recent theoretical and experimental studies of mineral physics have indicated that the MgSiO_3 perovskite, most abundant mineral in the Earth's lower mantle, undergoes an exothermic phase change to a post-perovskite (PPV) structure just above the core-mantle boundary (CMB). Since the PPV phase change is characterized by a steep Clapeyron slope, the phase transition is expected to have an important effect on the mantle dynamics. Here we study the influences of the PPV phase transition on the dynamics in the deep mantle by a three-dimensional model of mantle convection, with special emphasis to the influence on the thermal state in the lower mantle [Kameyama and Yuen, 2006].

A three-dimensional convection in a basally-heated rectangular box of 3000 km height and aspect ratio of $6 \times 6 \times 1$ is considered. The computational domain is divided uniformly into $512 \times 512 \times 128$ meshes based on a finite-volume scheme. The calculations are carried out by our newly developed code "ACuTEMan" for the Earth Simulator [Kameyama *et al.*, 2005, Kameyama, 2005]. We employed an extended Boussinesq approximation, where the effects of latent heat, adiabatic (de)compression and viscous dissipa-

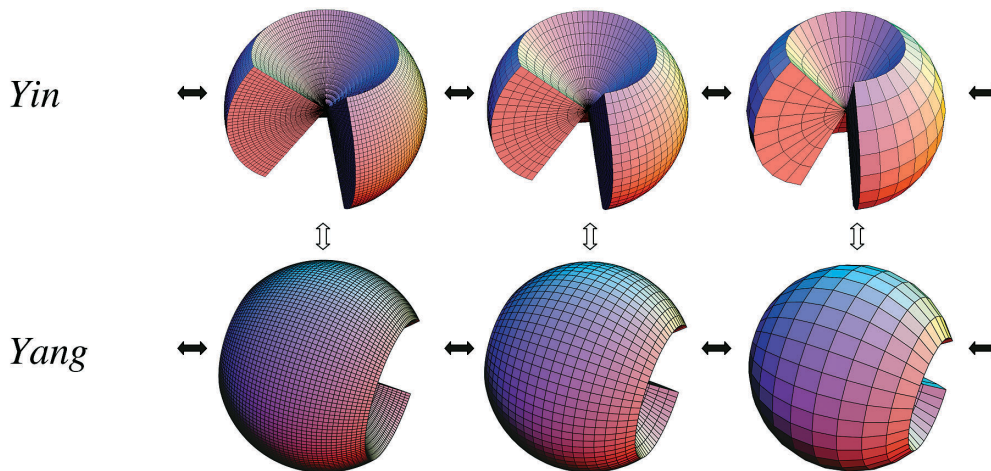


Fig. 2 The Yin-Yang multigrid method for the solution of the vacuum magnetic field potential. The full approximation storage algorithm is used. The horizontal boundary values of the Yin and Yang grids for the overset are determined by the mutual interpolation (white arrows) at the every grid level in the V-cycle of the multigrid method (gray arrows).

tion are explicitly included. The viscosity of mantle materials is assumed to be exponentially dependent on temperature and depth. We take into account the temperature-dependence of thermal conductivity, which mimics the effects of radiative heat transfer expected to be dominant in a hotter part of the mantle. In addition to the endothermic phase transition at around 660 km depth, the transition between perovskite and PPV phases is modeled as a highly exothermic (i.e., with steep positive Clapeyron slope) phase change located near the core-mantle boundary (CMB). The details of numerical model can be found in [Kameyama and Yuen, 2006]. In this study the influences of the PPV transition are studied by systematically varying two parameters: (i) Rb/Ra where Ra and Rb are the Rayleigh numbers based on the density change due to the thermal expansion and the PPV phase transition, respectively, and (ii) the temperature T_{CMB} at the bottom surface which determines the stability field of PPV phase around there through the relative positioning with the temperature of the PPV phase transition T_{int} at the CMB.

In Figure 3 we show for two cases (a) the three-dimensional distributions of lateral thermal anomalies $\delta T \equiv T - \langle T \rangle$, and (b) the plots against height z of the horizontally-averaged $\langle T \rangle$ (green), maximum T_{max} (red) and minimum T_{min} (blue) temperature at height z . The values of T_{max} and T_{min} roughly represent the temperature of ascending and descending flows, respectively. In these calculations $T_{\text{CMB}} < T_{\text{int}}$ is assumed and, hence, the PPV phase is dominant at the bottom surface. The values of Rb/Ra adopted in cases L00 and L10 are 0 and 1.25, respec-

tively. Namely, in case L00 the PPV transition does not affect the convective nature at all, while in case L10 the PPV transition is assumed to cause 10% density jump and, hence, the density jump is much larger than the theoretical and experimental estimate ($\approx 1.5\%$).

Figure 3 shows that the thermal state at depth is significantly influenced by a sufficiently large density jump associated with the PPV transition. The thermal state in case L10 is characterized by (i) a thick transition region (ranging about $0.1 \leq z \leq 0.3$) between the perovskite to PPV phases and (ii) the vertical profile of $\langle T \rangle$ bent toward the phase equilibrium relations over the depth range. This is due to the steep positive Clapeyron slope as well as the large density jump associated with the PPV transition. Because the Clapeyron slope is steep and positive, the PPV transition is allowed to occur over the broad range of pressure (or depth) according to the temperature variation. In addition, when a significant amount of latent heat is exchanged during the phase transition, the thermal state in the transition region tends to be controlled by the thermodynamic p - T condition, as in the cases with solid-liquid phase transitions in melt dynamics. Since the rate of latent heat exchange is proportional to the density jump of the phase transition (Rb), a significant amount of latent heat is exchanged in case L10 and, hence, the thermal state in the PPV transition region becomes close to the phase equilibrium condition.

From a series of calculations we found that the influence of the PPV transition is prominent only when Rb/Ra is suffi-

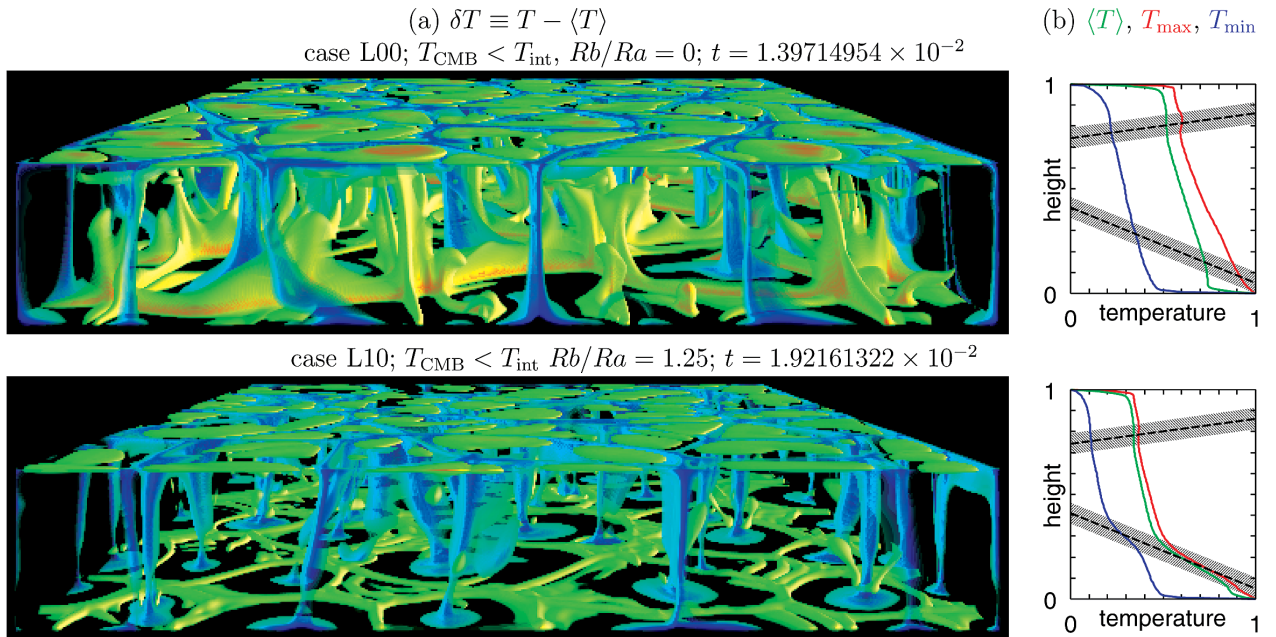


Fig. 3 Snapshots of convective flow patterns obtained for the two cases with $T_{\text{CMB}} < T_{\text{int}}$. Shown in (a) are the distributions of the lateral thermal anomaly δT . Indicated in blue are the cold anomalies with $\delta T \leq -0.05$, while in yellow to red are the hot anomalies with $\delta T \geq 0.025$. Plotted against nondimensional height z in (b) are the horizontally-averaged $\langle T \rangle$ (green), maximum T_{max} (red) and minimum T_{min} (blue) temperature at the height of z . Also schematically shown in (b) are the phase relations assumed in this calculation. For each phase transition, the thick dotted lines indicate the relations of phase equilibrium condition, while the hatched regions indicate the regions where the phase transition gradually occurs.

ciently large and T_{CMB} is lower than the temperature of the PPV transition T_{int} at the bottom surface. The former condition requires a sufficient amount of latent heat exchange during the phase transition, while the latter requires that the PPV transition takes place not only in cold but also in hot regions at depth. When the above conditions are met, the vertical temperature profile tends to be bent toward the equilibrium relations of the PPV transition owing to the buffering effect of latent heat exchange, as shown in Figure 3. We also found that, for realistic values of the density jump associated with the PPV transition ($\sim 1.5\%$), the transition is not likely to exert significant influences on the thermal state at depth.

3. Low-degree mantle convection in a spherical shell

Unlike mobile tectonic plates of the Earth, the surfaces of the Venus and Mars, often referred to "single-plate terrestrial planets", are covered by a thick immobile lithosphere or a cold stiff lid. The geodetic observations of Venus and Mars suggest that the thermal convection under the lid of these planets has relatively long-wavelength structure with the dominant spherical harmonic degrees of $\ell = 2 - 3$ or even lower. In particular, the crustal dichotomy of the Mars strongly implies that the convection in the Martian mantle is dominated by a structure of $\ell = 1$. However, such convective patterns are hardly compatible with those obtained by

earlier numerical and experimental studies of thermal convection with strongly temperature-dependent viscosity: The convection of stagnant-lid regime (for extremely strong temperature-dependence of viscosity) are always accompanied by a short-wavelength structure under a thick and immobile lid along the top cold surface. Here we numerically explore the possibility whether the improvement of viscosity model of the mantle material can help laterally elongate the convective structure under a highly viscous and immobile lid [Yoshida and Kageyama, 2006].

We consider a thermal convection of a Boussinesq fluid with infinite Prandtl number in a basally-heated 3-D spherical shell whose ratio of inner and outer radii is 0.55. The top and bottom surfaces of the spherical shell are assumed to be impermeable and the stress-free boundaries. Temperatures are fixed at the top and bottom surfaces. The governing equations are discretized by a second-order finite difference scheme on the Yin-Yang grid [Kageyama and Sato, 2004]. Other numerical details on the application of Yin-Yang grid to the simulation of the mantle convection can be also found in [Yoshida and Kageyama, 2004].

We focus on the effect of the depth-dependence in addition to the temperature-dependence of viscosity. We here assume two types of depth-dependence of viscosity: (1) the viscosity jumps at a certain depth corresponding to the

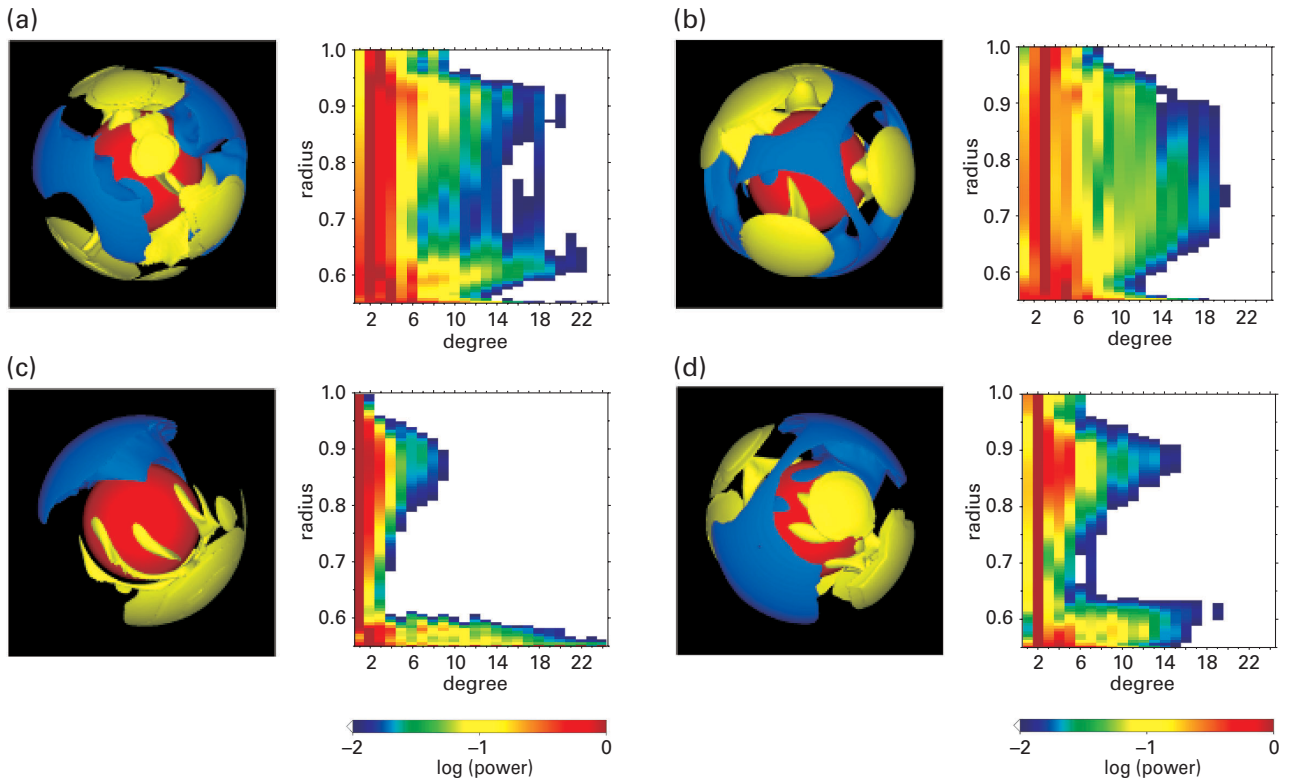


Fig. 4 The isosurface of lateral thermal anomaly δT and the power spectra of the spherical harmonics of temperature field at each depth. Sudden viscosity jumps of (a) 10^2 and (b) $10^{2.5}$ are imposed at the nondimensional radius $r = 0.9$, while exponential increases in viscosity with depth of (c) 10^2 and (d) $10^{2.5}$ are assumed for $0.55 \leq r \leq 0.9$. The yellow and blue isosurfaces indicate the hot and cold thermal anomalies, respectively. The plotted isosurfaces are $\delta T = \pm 0.25$ for (a) and (b), $\delta T = \pm 0.30$ for (c) and $\delta T = \pm 0.20$ for (d). The logarithmic power spectra are normalized by the maximum at each depth.

boundary between the upper and lower mantle of the Earth, and (2) the viscosity monotonously increases with depth in the Earth's lower mantle. Since there is no sufficient constraint for the actual viscosity contrast of the terrestrial planets due to the depth-dependence, we take it as a free parameter ranging from 30 to 300. We found that the combination of the strongly temperature- and depth-dependent viscosity causes long-wavelength structures of convection whose dominant spherical harmonic degrees are $\ell = 1 - 4$.

One of our important findings is that the degree-one convection can be easily reproduced when both the effects of the temperature- and depth-dependence on the viscosity are taken into account. Of course, the degree-one convection can take place solely with temperature-dependence of viscosity: A convection of "sluggish-lid" regime for a moderate temperature-dependence is characterized by long-wavelength convection cells under the slowly-moving lid. However, the sluggish-lid convection appears only in a narrow range of parameters depending on the viscosity contrast and the Rayleigh number. In contrast, the degree-one convection is realized in the wide range of viscosity contrast from 30 to 100 when the viscosity continuously increases with depth in the lower mantle. We thus speculate that the depth-dependence of viscosity is an important agent for understanding the nature of mantle convection in terrestrial planets.

4. Simulation of postseismic deformation

The Japan Islands are located in a subduction zone, where the Pacific plate is subducting beneath northeast Japan along the Kuril-Japan trenches, and the Philippine Sea plate descends beneath southwest Japan along the Nankai trough. In Japan, we have two types of large earthquakes which cause great disasters: one is the M 8-class great interplate earthquakes along trenches with a recurrence time of about 100 years, and the other is the M 7-class intraplate (inland) earthquakes on active inland faults with a recurrence interval longer than 1000 years. To simulate generation processes of these interplate and intraplate earthquakes in a complex system of interactive faults, one has to take strong heterogeneities of *elastic* and *viscoelastic* properties into account. The *elastic* structure beneath the Japan Islands is well determined owing to the recent geophysical surveys such as seismic tomography. On the other hand, the *viscoelastic* rheological structure, which strongly controls the interaction between earthquakes, is still unclear.

In Japan, nationwide geodetic surveys (leveling, triangulation and trilateration surveys) have been repeatedly carried out since 19th century. The 1896 *Riku-u* earthquake—an inland large (M7.2) event occurred in Tohoku region far from major plate boundaries—left clear long-term postseismic deformation in the nationwide leveling network.

Based on the postseismic deformation data following the

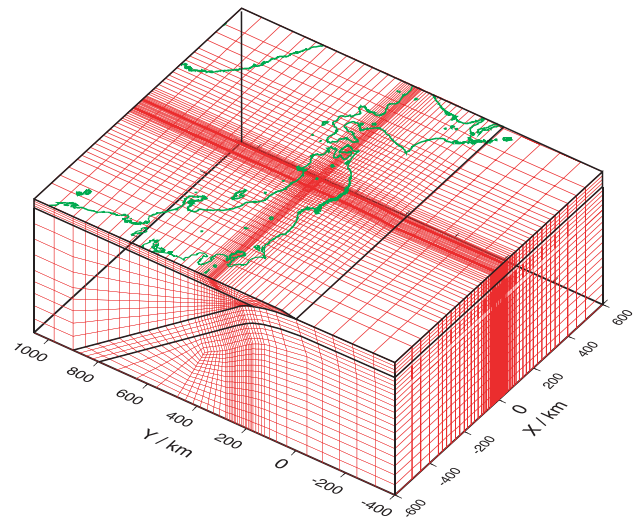


Fig. 5 FEM mesh used in postseismic deformation simulation. We assume that the crust and subducting Pacific plate are purely elastic, and the upper mantle is viscoelastic.

1896 *Riku-u* event, several researchers have estimated viscosity of the mantle wedge in the Tohoku region. In contrast to previous studies by Thatcher et al. (1980) and Suito and Hirahara (1999), we have included realistic distribution of elastic structure (the crust and subducting Pacific plate) in the calculation.

We use the finite element method with GeoFEM code for our viscoelastic simulation. Based on the plate configuration data deduced from the geophysical survey, we constructed FEM mesh shown in Fig. 5. [For GeoFEM simulation of earthquake simulation see also [Hyodo and Hirahara, 2004].] We assume that the crust and subducting Pacific plate are purely elastic, and the upper mantle is Maxwellian viscoelastic material. Imposing a static dislocation at the source area of *Riku-u* earthquake as the initial condition, we performed simulations of postseismic deformation due to the stress relaxation in the viscoelastic mantle. The elastic constants used in this study are the same as those used in Suito and Hirahara (1999).

Trying several simulations with different viscosity η , we found that the best estimate is $\eta = 1.40 \times 10^{19}$ [Pa·s]. The simulation with this value successfully reproduces the observed spatial profile of the height changes across the *Riku-u* rupture area and also reproduces the temporal profile of the nearest observational sites to the fault.

5. Summary

Based on our original tools—Yin-Yang grid and ACuTE method—we further developed our simulation models this fiscal year and applied them to the geodynamo and mantle convection simulations. We also developed an earthquake simulation model to estimate the upper mantle viscosity.

Byproducts of this fiscal year's research are; a pedagogical paper on rotating geophysical systems [Kageyama and Hyodo, 2006] and new grid system for dipole magnetic field [Kageyama et al., 2006].

References

- Hyodo, M., and K. Hirahara (2004), GeoFEM kinematic earthquake cycle simulation in southwest japan, *Pure Appl. Geophys.*, 161, 2069–2090.
- Kageyama, A. (2005a), Yin-Yang grid and geodynamo simulation, in *Computational Fluid and Solid Mechanics 2005*, edited by K. J. Bathe, pp.688–692, Elsevier, Cambridge, MA, USA, ISBN 0080444768 (Hardcover).
- Kageyama, A. (2005b), Dissection of a sphere and Yin-Yang grids, *J. Earth Simulator*, 3, 20–28.
- Kageyama, A., and M. Hyodo (2006), Eulerian derivation of the coriolis force, *Geochem. Geophys. Geosyst.*, 7(2), Q02009, doi:10.1029/2005GC001132, arXiv:physics/0509004.
- Kageyama, A., and T. Sato (2004), The "Yin-Yang Grid": An overset grid in spherical geometry, *Geochem. Geophys. Geosyst.*, 5(9), Q09005, doi:10.1029/2004GC000734, arXiv:physics/0403123.
- Kageyama, A., and M. Yoshida (2005), Geodynamo and mantle convection simulations on the Earth Simulator using the Yin-Yang grid, *J. Physics: Conference Series*, 16, 325–338, doi:10.1088/1742-6596/16/1/045, arXiv:physics/0506192.
- Kageyama, A., M. Kameyama, S. Fujihara, M. Yoshida, M. Hyodo, and Y. Tsuda (2004), A 15.2 tflops simulation of geodynamo on the earth simulator, in *Proceedings of ACM/IEEE Supercomputing Conference 2004 SC2004*, Pittsburgh, PA, USA, <http://www.sc-conference.org/sc2004/schedule/pdfs/pap234.pdf>.
- Kageyama, A., M. Kameyama, M. Yoshida, and M. Hyodo (2005), Computer simulations of geodynamo and mantle convection, *Annual Report of the Earth Simulator Center, April 2004-March 2005*, 133–138.
- Kageyama, A., T. Sugiyama, K. Watanabe, and T. Sato (2006), A note on the dipole coordinates, *Computers and Geosciences*, 32, 265–269, doi:10.1016/j.cageo.2005.06.006, arXiv:physics/0408133.
- Kameyama, M. (2005), ACuTEMan: A multigrid-based mantle convection simulation code and its optimization to the Earth Simulator, *J. Earth Simulator*, 4, 2–10.
- Kameyama, M., and D. A. Yuen (2006), 3-D convection studies on the thermal state in the lower mantle with post-perovskite phase transition, *Geophys. Res. Lett.*, 33, L12S10, doi:10.1029/2006GL025744.
- Kameyama, M., A. Kageyama, and T. Sato (2005), Multigrid iterative algorithm using pseudo-compressibility for three-dimensional mantle convection with strongly variable viscosity, *J. Comput. Phys.*, 206(1), 162–181, arXiv:physics/0410249.
- Yoshida, M., and A. Kageyama (2004), Application of the Yin-Yang grid to a thermal convection of a Boussinesq fluid with infinite Prandtl number in a three-dimensional spherical shell, *Geophys. Res. Lett.*, 31(12), L12609, doi:10.1029/2004GL019970, arXiv:physics/0405115.
- Yoshida, M., and A. Kageyama (2006), Low-degree mantle convection with strongly temperature- and depth-dependent viscosity in a three-dimensional spherical shell, *J. Geophys. Res.*, 111, B03412, doi:10.1029/2005JB003905.

地球ダイナモ、マントル対流、地震のシミュレーション

プロジェクト責任者

陰山 聡 海洋研究開発機構 地球シミュレータセンター

著者

陰山 聡^{*1}, 亀山 真典^{*1}, 吉田 晶樹^{*1}, 兵藤 守^{*1}, 古市 幹人^{*1}

^{*1} 海洋研究開発機構 地球シミュレータセンター

キーワード: 地球ダイナモ, マントル対流, ACuTE法, インヤン格子, 多重格子法

我々の最終的な目標は、地球シミュレータ(ES)を駆使した大規模計算機シミュレーションを通じて、地球ダイナモとマントル対流をはじめとする地球内部全体の構造とダイナミクスを理解することである。そのために必要となる大規模並列計算手法や基本数値アルゴリズムの独自開発にも積極的に取り組んでいる。

今年度はまず、我々が考案した独自の球面格子(インヤン格子)法をさらに発展させた。特に、球面を合同な2つの領域に分割する幾何学的問題(インヤン分割)と、一般化されたインヤン格子との関係を明らかにするとともに、マルチグリッド法をインヤン格子上で実装した。そしてこのプログラムを地球ダイナモの磁場の境界条件の改良に関する問題(数学的には単位球の外側領域のポテンシャル問題をノイマン境界条件で解く問題)に適用し、その精度と高速さを確認した。

マントル対流については、最近発見されたマントル最深部での相転移(ポストペロプスカイト相転移)がマントル対流に与える影響に注目した研究を行った。本研究ではポストペロプスカイト相転移を特徴づける熱力学的性質のうち、相転移に伴う密度変化、及び底面境界の温度とそこでの相転移温度との大小関係、の2つを系統的に変えてシミュレーションを行った。シミュレーションの結果から、ポストペロプスカイト相転移が深部の熱構造に顕著な影響を与えるのは、(i)相転移に伴う密度変化が極端に大きく、かつ(ii)底面境界の温度がそこでの相転移温度よりも低い場合に限られることが分かった。条件(i)は相転移の際に大量の潜熱が入り出す必要があることを意味し、(ii)はポストペロプスカイト相転移がマントル深部の広範な領域で起こることを要求している。これら2つの条件が満たされた場合には、強い潜熱の出入りが相転移領域の熱構造に大きく影響し、そこでの鉛直温度勾配がポストペロプスカイト相転移の温度・圧力条件から決まるものに近くなることも分かった。しかしながら、高温高圧実

験から見積られたポストペロプスカイト相転移の熱力学的性質と本研究結果とを照らし合わせると、実際のポストペロプスカイト相転移では相転移に伴う密度変化の大きさが十分ではなく、その結果下部マントルの熱構造に与える影響は非常に小さいことが示唆される。

また我々は、インヤン格子を用いた三次元球殻マントル対流シミュレーションコードを用いて、マントル物質の粘性率の温度依存性と圧力依存性について広範囲なパラメータ探索を行った。その結果、マントル対流層上下面の粘性率比が $10^4 \sim 10^5$ 以上の場合では、マントル表面を覆う低温かつ高粘性の境界層が発達する「スタグナント・リッド」型の対流パターンが得られた。スタグナントリッドの下のマントル対流はアスペクト比がほぼ1の非常に短波長な構造(次数6以上が卓越)で特徴づけられる。しかしながら、この短波長構造は地球及び他の地球型惑星のジオイド分布から推測される長波長構造の対流パターンとは異なる。そこでさらに上記の温度依存性の効果に加え、(i)マントルの粘性率がある深さ(地球の上部・下部マントル境界に相当する深さに設定)で急激に増加する場合と(ii)下部マントルの粘性率が深さに従って徐々に増加する場合の二種類の計算を行った。圧力依存性の程度により次数1~4が卓越する長波長構造の対流パターンが得られた。この「低次モード」のマントル対流パターンは地球及び他の地球型惑星で予想されている対流パターンに近いと思われる。特に(ii)の場合では、広範囲な圧力依存性の程度において次数1の対流パターンが得られた。これはプレートテクトニクスが存在しない火星のマントルで推測される次数1の対流パターンと矛盾しない。

我々はGeoFEMを用いた有限要素法コードを改良し、1896年の陸羽地震後の余効変動に関する観測データと、現実に近い粘弾性構造を取り入れたシミュレーションを比較することで上部マントルの粘性率の評価を行った。